Understanding the atmospheric circulations that lead to high particulate matter concentrations on the west coast of Namibia

Hanlie Liebenberg-Enslin[1*], Hannes Rautenbach[2,3], Reneé von Gruenewaldt[1], and Lucian Burger[1]

[1]Airshed Planning Professionals, Midrand, South Africa
[2]Climate Change and Variability, South African Weather Service, Pretoria, South Africa
[3]School of Health Systems and Public Health, University of Pretoria, South Africa

Abstract

Atmospheric circulations play a significant role in determining the extent and impact of local and regional air pollution. The Erongo Region, located in the western part of Namibia, falls within the west coast arid zone of southern Africa, and is characterised by low rainfall, extreme temperatures and unique climatic factors influencing the natural environment and biodiversity. Episodic dust storms, associated with easterly wind conditions, are common during austral autumn and winter months. During these events, dust is transported westwards over long distances across the Namibian continent towards the Atlantic Ocean. During 2017, such easterly wind conditions appeared to occur earlier and more frequently than in previous years. Of interest is that high PM_{10} concentrations (particulate matter with aerodynamic diameters of less than or equal to 10 micron) measured at the coastal towns of Swakopmund and Walvis Bay in the Erongo Region during 2017 were found to also coincide with south-westerly to north-westerly winds from the ocean during prevailing easterly wind events. In this study, the easterly wind events that occurred on 19 March 2017 and 6 July 2017 were assessed to investigate how local-scale coastal atmospheric circulation changes could have developed from the easterly wind conditions, and how such development could have contributed to wind direction deviations and the high PM_{10} concentrations measured at Swakopmund and Walvis Bay. It was found that in addition to the westward transport of PM_{10} from inland sources during easterly wind events, higher coastal concentrations of PM_{10} can also develop as a result of north-easterly / south-westerly wind conversion lines and the cyclonic circulation enhancement associated with easterly wind induced coastal troughs and coastal lows.

Keywords

Namibia, Erongo Region, air quality, particulate matter, wind patterns

Introduction

The Erongo Region is located in the western part of Namibia and is bounded by the Atlantic Ocean to the west and the continental escarpment to the east (approximately 180 km inland). From a hydrological perspective, the Erongo Region is drained in the central part by the deeply-incised Swakop and Khan Rivers, with the Kuiseb River separating the stony desert from the Namib sand dunes in the south (Tyson and Seely, 1980).

The Erongo Region falls within the west coast arid zone of southern Africa, and is characterised by low rainfall with extreme temperature ranges and unique climatic factors influencing the natural environment and biodiversity (Goudie, 2009). Episodic dust storms, associated with strong easterly wind conditions, are common during austral autumn and winter months. Associated dust is derived primarily from intermittent natural sources, giving rise to dust emissions only under conditions of high wind speeds. Windblown dust from natural sources is estimated to account between 75% (Ginoux et al., 2012) and 89% (Satheesh & Moorthy, 2005) of the global aerosol load, of which 25%

(Ginoux et al., 2012) to 50% (Tegen & Fung, 1995) is attributed to disturbed soil surfaces and the rest to natural soil surfaces. In Africa, approximately 54% of the dust is from desert and sparsely vegetated soils (Tegen & Fung, 1995). Anthropogenic sources account for 25% of global dust emissions (Ginoux et al., 2012). In the Erongo Region, anthropogenic sources of dust, such as unpaved roads, mining and exploration operations (primarily uranium prospecting), continuously contribute to atmospheric dust loads (Liebenberg-Enslin et al., 2010).

High concentrations of particulates in the air pose a risk to human health and welfare (Rashki et al., 2012; Rashki et al., 2013(a); Rashki et al., 2013(b)). Various studies have found a link between increased morbidity and mortality, especially amongst children and the elderly, and dust storm events (Ginoux et al., 2004; Karanasiou et al., 2012; De Longueville et al., 2013). In the Erongo region, radioactive dust associated with uranium mining and prospecting adds to the public concern (Liebenberg-Enslin et al., 2010).

Easterly wind events in the Erongo Region

During austral autumn and winter seasons, African continental anti-cyclonic circulation occasionally allows for easterly to north-easterly winds to descend along the downward slopes of the Namibian continent towards the Atlantic Ocean (Figure 1). This descend of air leads to a drop in air pressure as a result of vertical air column expansion, and the development of warm berg-wind conditions as a result of adiabatic heating. Although strong, hot and often uncomfortable for people, easterly wind conditions are usually relatively short lived[1].

During 2017, episodic dust storms associated with easterly wind events appeared to occur earlier and more frequently than in previous years. This heightened the public concern for high levels of radioactive dust from uranium prospecting and mining reaching the coastal towns of Swakopmund and Walvis Bay.
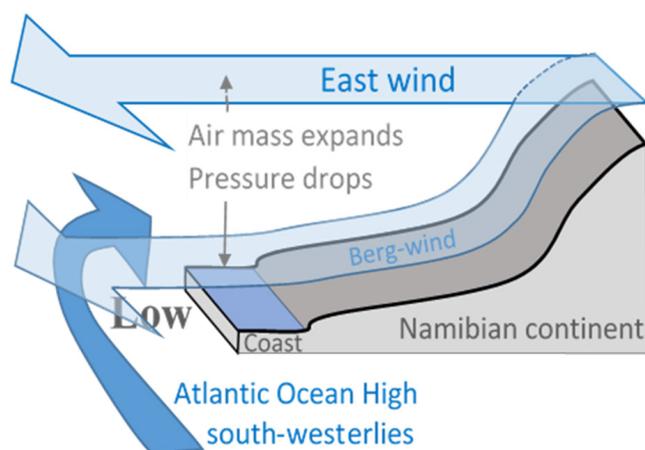

Figure 1: *Typical atmospheric flow characteristics during east wind conditions in Namibia. As berg-winds descends towards the coast, Mean Sea Level Pressures (MSLPs) drops to form either low pressure troughs or cut-off lows along the coastline. Because of the Coriolis force, such lows are associated with cyclonic (clockwise) circulation forcing.*

Although it is expected that fine particulates get lifted and carried across the interior of the Erongo Region towards the coast by easterly winds, easterly wind episodes that were monitored in 2017 indicated that high PM_{10} (Particulate Matter (PM) with an aerodynamic diameter of less or equal to 10 micron) concentrations recorded at Swakomund and Walvis Bay were also caused by PM_{10} that approached the towns from other directions than the prevailing easterly flow, which included onshore flow from south-westerly to north-westerly winds.

Of particular interest is that the high PM_{10} concentrations that were measured at the coastal towns of Swakopmund and Walvis Bay in the Erongo Region between 18 and 20 March 2017 were found to also coincided with south-westerly to north-westerly orientated winds during the prevailing easterly wind event, while wind direction deviations also occurred during the high PM_{10} concentration easterly wind event of 6 July 2017. While easterly wind conditions can explain the westward transport of PM_{10} from inland sources towards the Namibian coast, it is not clear why high PM_{10} concentrations were measured at the same

time under conditions of local-scale south-westerly to north-westerly wind directions, indicative of onshore flow from the Atlantic Ocean.

The purpose of this paper is to investigate how the local-scale atmospheric circulation deviations (south-westerly to north-westerly winds, in contrast to the large-scale prevailing easterly winds) observed on 19 March 2017, as well as 6 July 2017, could have developed from easterly wind conditions, and how these could have contributed to the high PM_{10} concentrations measured at Swakopmund and Walvis Bay.

Ambient air quality monitoring in the Erongo Region

Monitoring stations and parameters recorded

As part of the Strategic Environmental Management Plan (SEMP) initiated by the Namibian Ministry of Mines and Energy, an ambient monitoring network was established in the Erongo Region at the end of 2016 with the objective to measure PM_{10}, $PM_{2.5}$ and Radon concentrations. In addition, meteorological variables such as wind direction and speed, temperature, Relative Humidity (RH), solar radiation, barometric pressure and rainfall are also recorded at selected stations (Table 1). Monitoring locations were chosen based on the most populated areas in the region (i.e. towns, except for Jakalswater which serves as a background station). The towns identified were Swakopmund, Walvis Bay, Arandis and Henties Bay (Figure 2).

Figure 2: *Location of ambient air quality monitoring stations, meteorological stations and radon stations in relation to the mines and sensitive receptors.*

Ambient PM_{10} concentrations at Swakopmund and Walvis Bay are measured using Met One Instruments Model BAM 1020, designation for continuous PM monitoring. E-Samplers, a light-scatter Aerosol Monitor, are used to record PM_{10} concentrations at Henties Bay and Jakalswater and for $PM_{2.5}$ monitoring at Swakopmund and Walvis Bay. The E-Sampler at Jakalswater is fitted with a Met One Instrument measuring wind speed, wind direction and temperature. Met One weather stations at Swakopmund, Walvis Bay and Arandis are fitted with a wind speed sensor, wind direction vane, ambient air temperature

[1] http://www.raison.com.na

sensor, RH sensor, precipitation tipping bucket, as well as atmospheric pressure and solar radiation sensors.   The Swakopmund and Walvis Bay stations are enclosed, while it should be noted that the Walvis Bay station is on top of the Walvis Bay Civic Centre (approximately 9 m above ground level), whereas the Swakopmund Station is on top of a 3m structure at the Swakopmund waste water works.

Table 1: *Monitoring stations and parameters recorded*

Monitoring Location	Pollutant/ Parameter Measured									
	PM_{10}	$PM_{2.5}$	Wind Speed	Wind Direction	Temperature	Relative Humidity	Solar Radiation	Barometric Pressure	Rainfall	Radon
Swakop-mund	X	X	X	X	X	X	X	X	X	X
Walvis Bay	X	X	X	X	X	X		X		X
Arandis			X	X	X	X	X	X	X	X
Henties Bay	X			X	X			X		
Jakalswa-ter	X		X	X	X	X		X		

Prevailing wind fields in the Erongo Region

The wind fields of the Erongo Region are influenced by a combination of synoptic and local scale circulations. Wind directions in the central-northern parts of the region are predominantly from the east, northeast and southwest, where the easterly and north-easterly winds (eastern wind conditions) are often being associated with high wind speeds. Along the coast, southerly to south-westerly wind directions are modulated by the Atlantic Ocean anti-cyclonic circulation as well as temperature and pressure gradients that are orientated parallel to the coastline between the upwelling Benguela ocean-current and the warm arid continent. During the period between November 2016 and April 2017, wind speeds in the region were found to be mostly between 0 m.s^{-1} to 10 m.s^{-1}. Inland, at Arandis, prevailing west-south-westerly winds dominated, while at Jakalswater, the prevailing winds were east-north-easterly (Figure 2). Easterly winds, associated with berg-wind conditions, were recorded for 22% of the period between November 2016 and April 2017 at Jakalswater, 16% at Arandis, 9% at Swakopmund and 10% at Walvis Bay. Easterly wind conditions were most prevalent during the month of March 2017, occurring for 32% of the time at Arandis and 41% at Jakalswater. At the coast, easterly flow was recorded at 9% and 10% of the time at Swakopmund and Walvis Bay, respectively.

During east wind conditions, high wind speeds of up to 22 m.s^{-1} were recorded at the Namibian coast. These strong

winds are occasionally also being associated with south-westerly to north-westerly wind directions during east wind conditions at the towns of Swakopmund and Walvis Bay.

Case studies of easterly winds and high PM_{10} concentrations

Easterly wind event on 6 July 2017

Easterly berg-wind conditions prevailed across the Erongo Region on 6 July 2017. At Swakopmund wind directions were easterly from 00:00 to 09:00, from where it changed to north-easterly between 09:00 to 14:00 (Figure 4a). A significant change in wind direction appeared at 16:00 when a north-easterly wind developed. Shortly after this, the wind direction gradually returned to easterly winds in the later afternoon towards 24:00. On the same day, PM_{10} concentrations were mostly below 50 µg.m^{-3}. However, during the time interval when the winds turned to north-easterly (09:00-14:00), a significant increase in PM_{10} with a maximum of 312 µg.m^{-3} at 10:00 developed, most probably from sources to the north-east of Swakopmund. It is interesting to note that the PM_{10} concentration peak of 312 µg.m^{-3} that occurred at Swakopmund is significantly higher than the six-month average (data for the period November 2016 to April 2017) which ranged between 30 µg.m^{-3} (Swakopmund) and 35 µg.m^{-3} (Walvis Bay).

Figure 3: *Daily PM_{10} and $PM_{2.5}$ concentrations at (a) Swakopmund and (b) Walvis Bay with average daily wind directions indicated for the month of July 2017.*

At Walvis bay (Figure 4b), the wind direction pattern was very

similar to what was recorded at Swakopmund, where the significant wind direction change at 16:00 was also captured, while PM_{10} concentrations were mostly around 10 μg.m^{-3}, but also slightly increased to 132 μg.m^{-3} with the change in wind direction towards north-east when the concentration peak was recorded at Swakopmund.
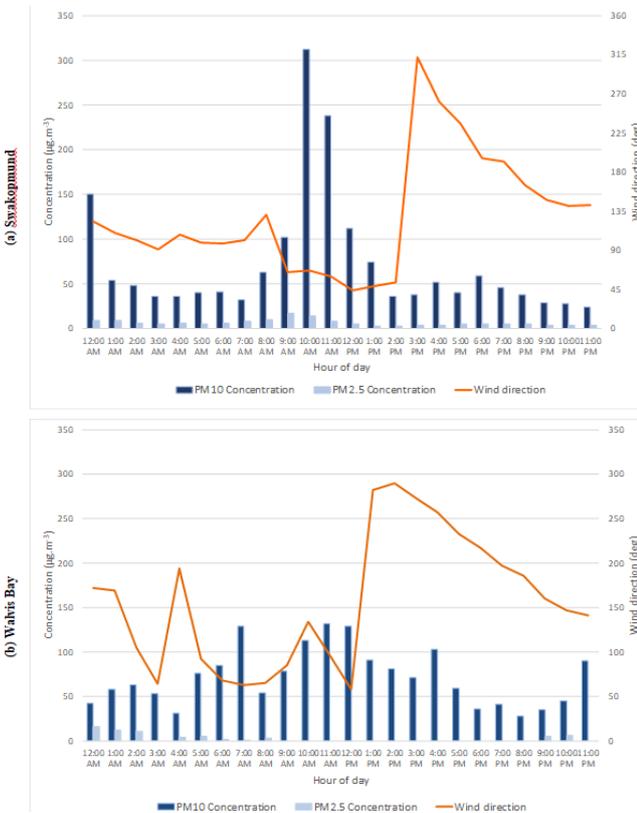

Figure 4: *Hourly PM_{10} and $PM_{2.5}$ concentrations at (a) Swakopmund and (b) Walvis Bay with average hourly wind directions indicated for 6 July 2017.*

Daily PM_{10} concentrations for the month July 2017 are presented as polar plots[2] in Figure 5. Polar plots represent the concentration in relation to the wind direction and wind speed from where it originated. At Swakopmund, high PM_{10} concentrations were recorded during higher wind speeds episodes (>8 m.s^{-1}) from the east-north-east, and during lower wind speeds (4-6 m.s^{-1}) from the east-south-east. Similarly, high PM_{10} concentrations at Walvis Bay occurred during strong east-north-easterly winds (>6 m.s^{-1}) with lower PM_{10} concentrations under higher wind speeds from the south and south-south-west. It therefore appears as if PM_{10} sources for Swakopmund are located to the north-west to south-south-west of the monitoring station, whereas for Walvis Bay sources might be located to the south-south-west to south-east of the station.

Polar plots for hourly PM_{10} concentrations on 6 July 2017 reflect the highest PM_{10} concentrations during strong east-north-easterly winds at both Swakopmund and Walvis Bay (Figure 6). Swakopmund recorded higher PM_{10} concentrations under

these higher wind speeds than at Walvis Bay (highest hourly PM_{10} concentration of 312 μg.m^{-3} and maximum wind speed of 18.2 m.s^{-1} at Swakopmund compared to the highest PM_{10} concentration of 132 μg.m^{-3} and maximum wind speed of 7.6 m.s^{-1} at Walvis Bay). Lower PM_{10} contributions were associated with south and south-westerly winds at the Swakopmund station, and south-west to north-westerly winds at the Walvis Bay station.
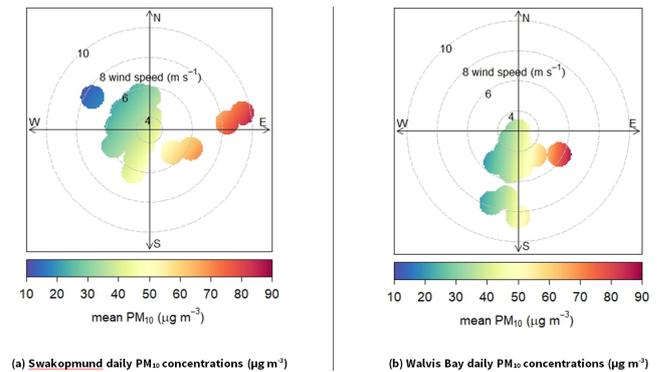

Figure 5: *Daily PM_{10} concentrations as polar plots for (a) Swakopmund and (b) Walvis Bay for the month of July 2017.*
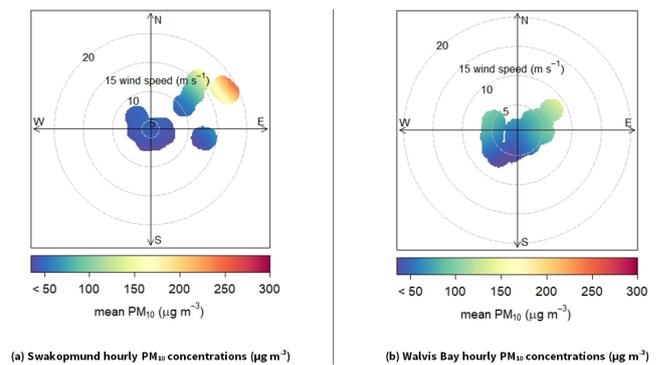

Figure 6: *Hourly PM_{10} concentrations as polar plots for (a) Swakopmund and (b) Walvis Bay for 6 July 2017.*

European Reanalysis Interim (ERA-Interim) data (Dee at al., 2011) were downloaded to produce wind and sea-level pressure maps for 00:00, 06:00, 12:00 and 18:00 Greenwich Mean Time (GMT) on 6 July 2017 (Figures 7a, 7b, 7c and 7d). According to these maps, north-easterly winds were observed between the Namibian escarpment and coastline, with the Botswana anti-cyclone well-established to the east of the country.

As the east wind descended from the Namibian interior towards the coast, the vertical air mass expanded and air pressures decreased to form higher pressures along the escarpment to lower pressures along the coast (illustrated in Figure 1 and observed in Figures 7a, 7b, 7c and 7d). As a result, a trough associated with lower pressures developed along the Namibian coast line.

In this trough, Mean Sea Level Pressure (MSLP) values at Swakopmund and Walvis Bay were in the order of 1019 hPa at

[2] R package for air quality data analysis (Carslaw & Ropkins, 2012) and the Openair version 0.8 0 (Carslaw, 2013).

00:00 GMT. Pressures increased towards 06:00 to values of 1020 hPa. I noticeable drop in MSLP to 1017 hPa occurred between 06:00 GMT and 12:00 GMT, from where MSLPs stabilised towards 18:00 GMT at 1017 hPa.

While north-easterly winds prevailed at the two towns at 00:00 GMT, 06:00 GMT and 18:00 GMT, the deepening of the trough reflected for 12:00 GMT (Figure 7c) resulted in cyclonic (clockwise) circulation enhancement (north-eastern to the east of the trough and south-western to the west of the trough), which could explain the noticeable change in wind direction towards a north-westerly direction at 16:00 – as reflected in the weather station data (Figures 4a and 4b). The cyclonic circulation enhancement that appeared on 6 July 2017, however, did not result in exceptionally high PM_{10} concentrations. The high concentrations that were observed earlier in the day may rather be attributed to an upwind source towards the northeast.
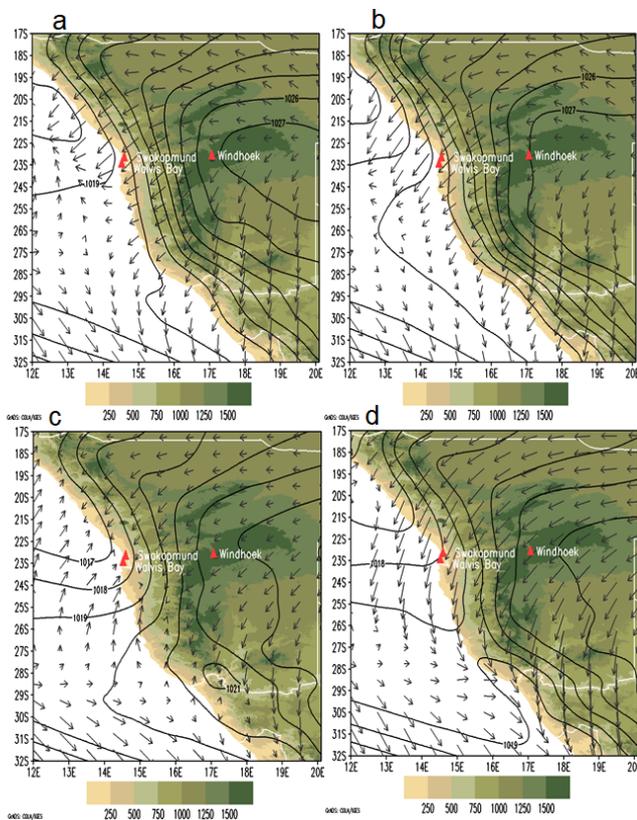

Figure 7: Map of Mean Sea Level Pressure (MSLP) (contours) and 10m wind vectors at 00:00, 06:00, 12:00 and 18:00 Greenwich Mean Time: GMT (a, b, c, d, respectively) on 6 July 2017. Topography (meters above mean sea level) is shaded, while the positions of Windhoek, Swakopmund and Walvis Bay are indicated by red triangles.

Easterly wind event on 19 March 2017

Easterly wind conditions were prevalent during March 2017, occurring for 32% of the time at inland stations of Arandis and 41% at Jakalswater. At the coast, easterly flow was recorded for 9% at Swakopmund and 10% at Walvis Bay. High PM_{10} concentrations were recorded on 18, 19, 20, 24, 25, 30 and 31 March 2017 at Swakopmund and Walvis Bay (Figure 8). On these days, easterly wind conditions prevailed inland at Jakalswater
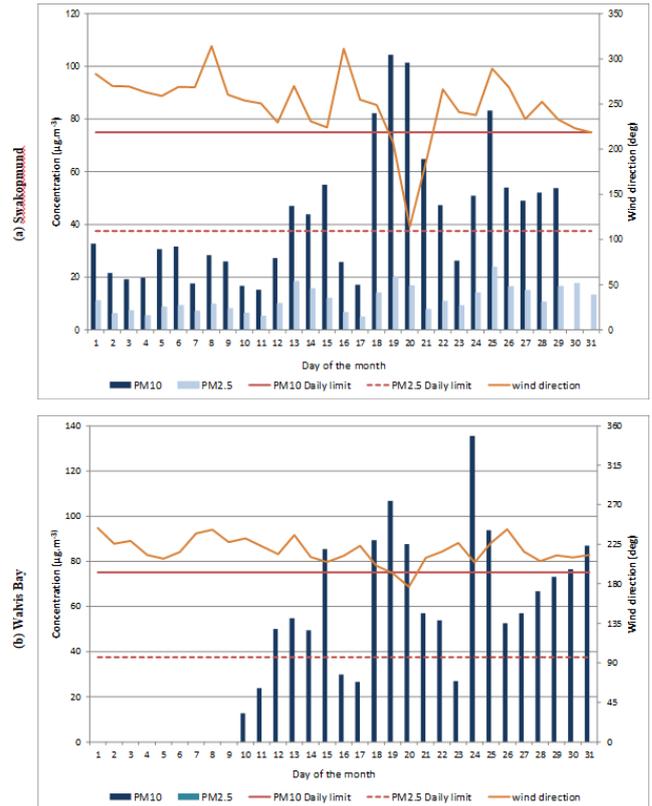

Figure 8: Daily PM_{10} and $PM_{2.5}$ concentrations for (a)Swakopmund and (b) Walvis Bay with average daily wind direction indicated for the month of March 2017.
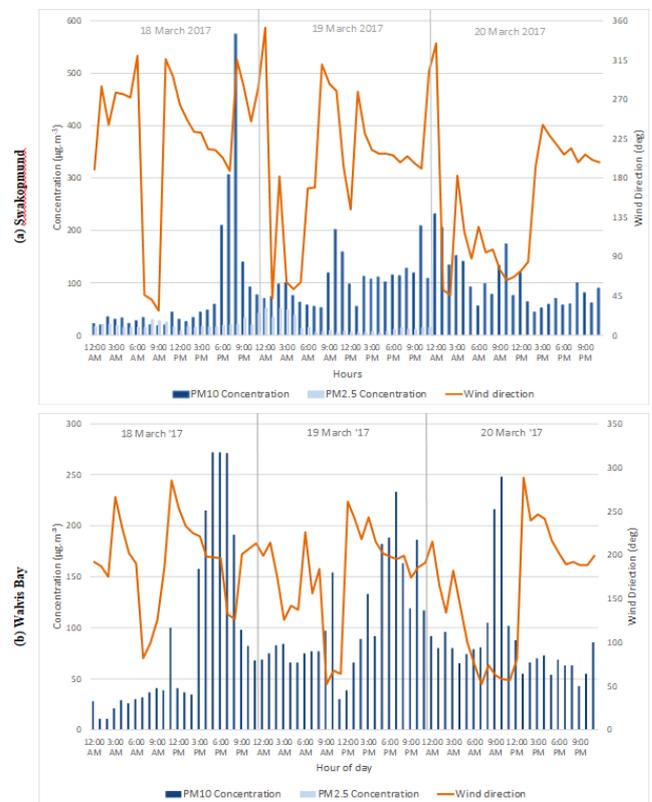

Figure 9: Hourly PM_{10} and $PM_{2.5}$ concentrations for (a) Swakopmund and (b) Walvis Bay with average hourly wind direction indicated for 19 and 20 March 2017.

and Arandis, but at Swakopmund and Walvis Bay high hourly PM$_{10}$ concentrations recorded between the late hours of 18 March and the early hours of 20 March were mainly associated with southerly to south-westerly winds. The highest and third highest hourly PM$_{10}$ concentrations recorded at Swakopmund of 575 µg.m^{-3} (20:00 on 18 March 2017) and 232 µg.m^{-3} (12:00 on 20 March 2017) were, however, recorded when the wind was from the north-west (Figure 9).

During the early hours of 19 March 2017 (the focus period for this study), wind directions at Swakopmund returned from north-west to easterly winds (Figure 9a). At 08:00 the wind direction turned to north-west in a very short time period, and maintained this direction until 13:00, from where south-westerly winds developed during most of the afternoon. Late at night, just before 12:00, the wind direction again changed to north-east over a relative short period. At Walvis Bay (Figure 9b), the changes in wind direction was not as extreme as observed at Swakopmund. Nevertheless, north-westerly winds with high PM$_{10}$ concentrations developed from just before 12:00. What is interesting is that the north-westerly winds were all associated with higher PM$_{10}$ concentrations at both Swakopmund and Walvis Bay.

Daily PM$_{10}$ concentrations, presented as polar plots for the month of March 2017, indicate windblown dust under high wind speeds of 8 m.s^{-1} (Swakopmund) and 8 to 10 m.s^{-1} (Walvis Bay). At Swakopmund, these concentrations were recorded during east-south-easterly and south to south-south-westerly winds, and south-south-westerly winds at Walvis Bay (Figure 10). The highest hourly concentrations at Walvis Bay were mainly associated with south-south-westerly winds (Figure 10). On average, higher hourly PM$_{10}$ concentrations and higher wind speeds were recorded at Swakopmund compared to Walvis Bay during 18 to 20 March 2017. From the highest PM$_{10}$ concentration measurements were made during onshore south-west to north-west winds (from the Atlantic Ocean) at both Swakopmund and Walvis Bay.

Highest hourly PM$_{10}$ concentrations for the period 18 to 20 March 2017, depicted as polar plots in Figure 11, show a combination of high PM$_{10}$ concentrations associated with east-north-easterly to south-south-westerly winds at both Swakopmund and Walvis Bay. Although the expected easterly wind signature is present, higher PM$_{10}$ concentrations resulted from winds from the Atlantic Ocean. The highest hourly PM$_{10}$ concentration (575 µg.m^{-3}) recorded at Swakopmund over these three days was under moderate winds (5 m.s^{-1}) from the north-west. The second highest PM$_{10}$ concentration (307 µg.m^{-3}) was during south-south-westerly winds at 6.4 m.s^{-1}. At Walvis Bay, the highest hourly PM$_{10}$ concentration recorded was 272 µg.m^{-3} over two (2) hours when the wind was from the south-south-west blowing at moderate velocities (9.4 and 7.6 m.s^{-1}).

European Reanalysis Interim (ERA-Interim) data (Dee at al., 2011) were downloaded to produce wind and sea-level pressure maps for 00:00, 06:00, 12:00 and 18:00 Greenwich Mean Time (GMT) on 19 March 2017 (Figures 12a, 12b, 12c and 12d). As
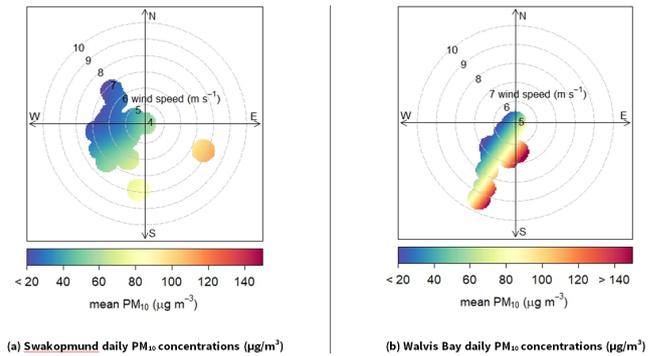

Figure 10: *Daily PM$_{10}$ concentrations as polar plots for (a) Swakopmund and (b) Walvis Bay for the month of March 2017.*
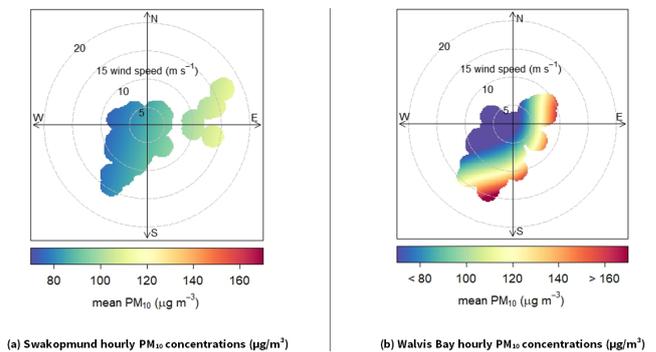

Figure 11: *Hourly PM$_{10}$ concentrations as polar plots for (a) Swakopmund and (b) Walvis Bay for 18 to 20 March 2017.*

the easterlies blows towards the Namibian coastline from the higher escarpment, air pressures dropped, as indicated by isobars that are almost parallel to the coastline in the area west of the high escarpment, which had led to the development of a coastline trough. In general, north-easterly conditions were observed in the Swakopmund / Walvis Bay area at 00:00 GMT. With these north-easterlies, strong Atlantic Ocean anti-cyclonic south-westerly winds appeared to allow for a north-easterly / south-westerly wind conversion line to develop along the coast of Namibia. A coastal-low feature which is an extension of the coastal through is also visible at 00:00 GMT (Figure 12a). Signs of cyclonic circulation is visible around the coastal-low, which developed even further towards 06:00 GMT as MSLPs dropped from 1013 hPa to 1011 hPa (Figure 12b). Wind directions also changed from northeast to southwest between 00:00 GMT and 06:00 GMT, which is also indicative of cyclonic circulation enhancement, which form part of the north-easterly / south-westerly wind conversion line. At 12:00 GMT, north-westerly winds develop with a significant increase in PM$_{10}$ concentrations, especially at Swakopmund (Figure 12c).

The change in wind direction from northeast to southwest to northwest can be interpreted as cyclonic circulation along the coast of Swakopmund and Walvis Bay, associated with the clockwise recirculation of PM$_{10}$. At the same time, the north-westerly / south-easterly wind conversion line would have prevented PM$_{10}$ to be dispersed westwards towards the deeper Atlantic Ocean, which could also have contributed to the accumulation of PM$_{10}$ along the coast that was recirculated
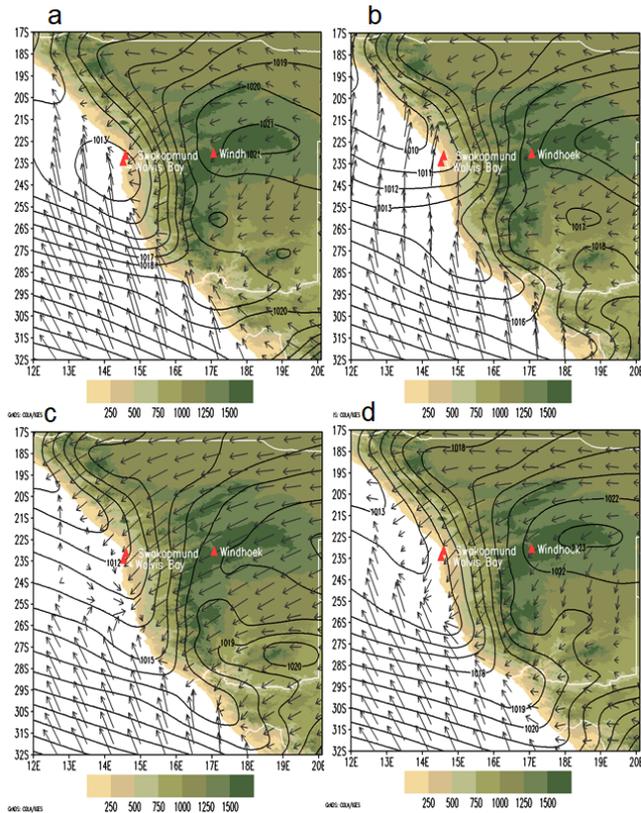
Figure 12: *Map of Mean Sea Level Pressure (MSLP) (contours) and 10m wind vectors at 00:00, 06:00, 12:00 and 18:00 Greenwich Mean Time: GMT (a, b, c, d, respectively) on 19 March 2017. Topography (meters above mean sea level) is shaded, while the positions of Windhoek, Swakopmund and Walvis Bay are indicated by red triangles.*

back towards the continent by north-westerly winds to generate conditions of exceptionally high PM_{10} concentrations, as indicated by the 12:00 GMT map (Figure 12c) as well as the high PM_{10} concentrations measured at Swakopmund (and Walvis Bay) (Figure 12a) between 08:00 and 13:00 on 19 March 2017.

Characterisation of likely dust sources

Filter tape from the PM_{10} BAM 1020 samplers at Swakopmund and Walvis Bay were analysed using Inductively Coupled Plasma - Mass Spectrometry (ICP-MS) for elemental content (43 elements) in an attempt to differentiate between the main sources contributing of high hourly PM_{10} concentrations at Swakopmund and Walvis Bay. Both towns border the Atlantic Ocean to the west and the desert gravel plains to the east, with the Kuiseb River mount and Namib Desert to the south of Walvis Bay. The main anthropogenic sources within the gravel plains of the Erongo Region are unpaved roads and mining and exploration activities (mainly uranium prospecting). Particulate matter from these areas reaching the coastal towns are wind dependent (windblown dust) whereas wind independent sources closer to the monitoring stations are likely to the associated with vehicle emissions, small boilers and hospital incinerators, and harbour activities at Walvis Bay.

ICP analysis was done for 43 elements on samples representing hours with high PM_{10} concentrations during the two case studies

– 6 July 2017 and 18 to 20 March 2017. Specific hours were selected reflecting the predominant wind direction during each case study as to eliminate dust from other directions during these periods.

For the 6th of July 2017 case study, 22 hours were selected from the Swakopmund station reflecting winds from the east-north-east to south-east (01:00 to 14:00 on 6 July and 04:00 to 11:00 on 7 July 2017). The main elements are presented in Table 2 and Figure 13. No filter tape was available from Walvis Bay for this period.

Table 2: *Elemental composition as percentages of the various samples*

| Sample ID	Swakopmund		Swakopmund		Walvis Bay	
	06 July 2017		18-20 March 2018		18-20 March 2018	
Element	(mg/ sample)	(%)	(mg/ sample)	(%)	(mg/ sample)	(%)
Arsenic, As	0.0007	1%	0.0010	1%	0.0000	0%
Iron, Fe	0.0122	26%	0.0122	16%	0.0177	38%
Magnesium, Mg	0.0012	3%	0.0074	10%	0.0083	18%
Manganese, Mn	0.0002	0%	0.0002	0%	0.0006	1%
Phosphorus, P	0.0010	2%	0.0019	3%	0.0000	0%
Selenium, Se	0.0001	0%	0.0004	1%	0.0002	0%
Sulphur, S	0.0165	35%	0.0524	69%	0.0195	41%
Titanium, Ti	0.0004	1%	0.0007	1%	0.0009	2%
Vanadium, V	0.0000	0%	0.0001	0%	0.0000	0%
	0.0322		0.0765		0.0471	
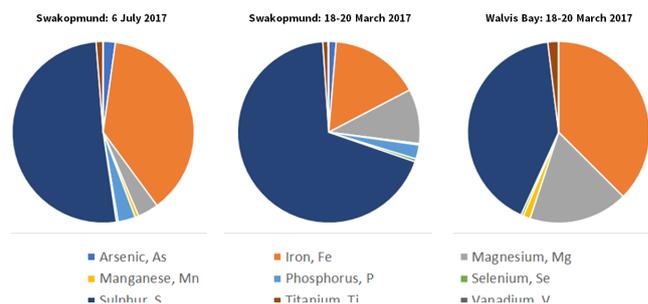
Figure 13: *Elemental composition of the samples from the case studies.*

Samples covering 25-hours from the Swakopmund station (06:00 to 23:00 on 18 March; 09:00 to 23:00 on 19 March and 00:00 to 04:00 on 20 March 2017) were analysed reflecting predominantly south-south-westerly to north-westerly winds during the period 18 to 20 March 2017. At Walvis Bay 15 hours (15:00 to 20:00 on 18 March and 15:00 to 23:00 on 19 March 2017) were selected reflecting similar wind directions. The main elements are presented in Table 2 and Figure 13.

The main elements from all three sample batches were arsenic (As), iron (Fe), magnesium (Mg), manganese (Mn), phosphorus (P), selenium (Se), sulphur (S), titanium (Ti) and vanadium (V). During the July east winds, sulphur (51%) and iron (38%) were more pronounced in the samples from Swakopmund, with lower fractions of 4% Mg and 3% P, respectively. For the two sites during the March case study, S and Fe remained the main elements (69% S from Swakopmund and 41% from Walvis Bay, and 16% Fe from Swakopmund and 38% from Walvis Bay). The Mg fraction was higher during these predominantly south-south-westerly to north-westerly winds (10% at Swakopmund and 18% at Walvis Bay). Elements associated with sea water are predominantly sodium (Na) and chloride (Cl), followed by Mg, V, S, calcium (Ca) and potassium (K) (https://en.wikipedia. org/wiki/Seawater). Elements associated with desert dust are mainly Ca, silica (Si), aluminium (Al), and some traces of Na and Mg (Rashki et al., 2012).

No clear distinction could be made in the chemical composition of the three sample batches from the two case studies where high PM_{10} concentrations were recorded. The expectation would have been that under predominant easterly winds (6th of July 2017 case study), the elements mostly associated with desert dust would dominate; whilst under prevailing south-westerly to north-westerly winds (between 18 and 20 March 2017), elements associated with the ocean would alternatively have dominated. Instead, the similar elemental composition of the PM_{10} samples indicates sources of possibly similar origin. All three samples show strong sea water signatures with some traces of desert dust. This is supported by the cyclonic circulation along the coast of Swakopmund and Walvis Bay, associated with the clockwise recirculation of PM_{10} back towards the continent by north-westerly winds.

Conclusions and recommendations

Two case studies, one between 18 and 20 March 2017 and the other on 6 July 2017, were considered to assess the atmospheric circulation patterns associated with the easterly wind conditions resulting in high PM_{10} concentrations at Swakopmund and Walvis Bay along west coast of Namibia. It was found that although easterly wind conditions prevailed over the Namibian continent, extensive temporal wind direction changes were observed at the Swakopmund and Walvis Bay coastline. Through further investigation it was concluded that in addition to the westward transport of PM_{10} from inland sources during easterly wind events, higher coastal concentrations of PM_{10} can also develop as a result north-easterly / south-westerly wind conversion lines as well as cyclonic circulation or cyclonic circulation enhancement, with the recirculation of PM_{10}, associated with coastal troughs and coastal lows. The study found a relationship between the (1) coastward decrease in continental air pressures due to easterly wind conditions, (2) the resultant development of coastal troughs (and sometimes coastal-lows), (3) the consequent development of conversion lines, (4) extensive changes in wind speed and direction, and (5) the high concentrations of PM_{10} concentrations (both as a result wind conversion line blocking and cyclonic recirculation) at Swakopmund and Walvis Bay. This is further confirmed by the

similarity in elemental content of dust sources under various prevailing wind conditions.

However, these findings need further investigation, especially on the meso-scale, which will not only provide lead to an improved understanding of local wind behaviour, but also local PM_{10} variation characteristics along the coastline of Namibia and the main contributing sources.

Acknowledgements

References

Carslaw, D. C. & Ropkins, K., 2012. Openair — an R package for air quality data analysis. Environmental Modelling & Software, 27 28, 52 61.

Carslaw, D. C., 2013. The openair manual — open source tools for analysing air pollution data. Manual for version 0.8 0, 14 February 2013, London: King's College CEPA/FPAC Working Group, 1998Colls, 2002.

De Longueville, F., Ozer, P., Doumbia, S. and Henry, S., 2013. Desert dust impacts on human health: an alarming worldwide reality and a need for studies in West Africa. International Journal of Biometeorology, 57, 1-19.

Dee, D. P., Uppala, S. M., Simmons, A. J., Berrisford, P., Poli, P., Kobayashi, S., Andrae, U., Balmaseda, M. A., Balsamo, G., Bauer, P., Bechtold, P., Beljaars, A. C. M., van der Berg, L., Bidlot, J., Bormann, N., Delsol, C., Dragani, R., Fuentes, M., Geer, A. J., Haimberger, L., Healy, S. B., Hersbach, H., Hólm, E. V., Isaksen, L., Kållberg, P., Köhler, M., Matricardi, M., McNally, A. P., Monge-Sanz, B. M., Morcrette, J.-J., Park, B.-K., Peubey, C., de Rosnay, P., Tavolato, C., Thépaut, J.-N. and Vitart, F. (2011), The ERA-Interim reanalysis: configuration and performance of the data assimilation system. Q.J.R. Meteorol. Soc., 137: 553–597. doi: 10.1002/qj.828

Goudie, A. S., 2009. Dust storms: Recent developments. Journal of Environmental Management, 90, 89–94.

Ginoux, P., Prospero, J. M., Torres, O. and Chin, M., 2004. Long term simulation of global dust distribution with the GOCART model: correlation with North Atlantic Oscillation. Environmental Modelling and Software, 19, 113 128.

Ginoux, P., Prospero, J. M., Gill, T. E., Hsu, N. C., and Zhao, M., 2012. Global-scale attribution of anthropogenic and natural dust sources and their emission rates based on MODIS Deep Blue aerosol products. Reviews of Geophysics, 50, RG3005, doi:10.1029/2012RG000388.

Karanasiou, A., Moreno, N., Moreno, T., Viana, M., de Leeuw, F., Querol, X., 2012. Health effects from Sahara dust episodes in Europe: literature review and research gaps. Environment International, 15, 107-114.

Liebenberg Enslin, H., Krause, N. & Breitenbach, N., 2010. Strategic Environmental Assessment for the Central Namib 'Uranium Rush Air Quality Specialist Report. Report APP/09/MME 02 Rev0 to the Ministry of Mines and Energy, Namibia.

 MME, 2017. Advanced Air Quality Management for the Strategic Environmental Management Plan for the Uranium and Other Industries in the Erongo Region: Ambient Air Quality Monitoring Report for the Period 1 November 2016 to 30 April 2017. Done on behalf of the Namibian Ministry of Mines and Energy. Report No. 16MME01-2.

Rashki, A., Eriksson, P.G., Rautenbach, C.J.deW., Kaskaoutis, D.G., Grote, W. and Dykstra, J., 2012. Assessment of chemical and mineralogical characteristics of airborne dust in the Sistan region, Iran. *Chemosphere*, 90, 227-236.

Rashki, A., Rautenbach, C.J.deW., Eriksson, P.G., Kaskaoutis, D.G. and Gupta, R., 2013(a). Temporal changes of particulate concentration in the ambient air over the city of Zahedan, Iran. *Air Quality, Atmosphere & Health*, 6, DOI 10.1007/s11869-011-0152-5, 123-135.

Rashki, A., Kaskaoutis, D.G., Eriksson, P.G., Rautenbach, C.J.deW, Flamant, C. and Abdi Vishkaee, F., 2013(b) Spatio-temporal variability of dust aerosols over the Sistan region in Iran based on satellite observations. *Natural Hazards and Earth System Sciences*, Volume 71, Issue 1, pp 563–585. DOI 10.1007/s11069-013-0927-0.

Satheesh, S. K. & Moorthy, K. K., 2005. Radiative effects of natural aerosols: a review. *Atmospheric Environment*, 39, 2089–110.

SAWS, 2017. Derived from Daily Synoptic Maps of the South African Weather Service (SAWS) http://www.weathersa.co.za/observations/synoptic-charts.

Tegen, I. & Fung, I., 1995. Contribution to the atmospheric mineral aerosol load from land surface modification. *Journal of Geophysical Research*, 100, 18707 18726.

Tyson, P.D., and Seely, M.K., 1980: Local winds over the Central Namib. *The South African Geographical Journal*, Vol. 62, No. 2, pp 135-150. September 1980.